Magnetic Field Control of the Back-Electron-Transfer Process Following Photoinduced Electron Transfer (PIET) in Biphenyl/Phenylpyrylium Salts in SDS Micellar Medium†

Mintu Halder,‡,§ Partha Pratim Parui,‡ K. R. Gopidas,# Deb Narayan Nath,‡ and Mihir Chowdhury*,‡

Department of Physical Chemistry, Indian Association for the Cultivation of Science, Jadavpur, Kolkata 700 032, India, and Photochemistry Research Unit, Regional Research Laboratory, Trivandrum 695 019, India

Received: July 6, 2001; In Final Form: December 12, 2001

Magnetic field effect (MFE) on the radical pairs (RPs) generated by the photoexcitation of the phenyl pyrylium ion (PP^+) in the presence of the electron donor biphenyl has been investigated. A large effect was observed particularly for the BP/PP^+ (**I**) case; the escape yield at 5 T was more than 20 times the zero-field value at a long time delay. The low-field variation of MFE conforms to the pattern expected for the isotropic HFC (hyperfine coupling) mechanism, and the high-field variation conforms to that expected for the relaxation mechanism. The addition of salt causes saturation at a slightly lower field, presumably because of a change in the rotational correlation time (local motion) of $PP^{\bullet}$ at the micellar surface. Introduction of a methyl group in the acceptor reduces the MFE considerably the reason for which is not immediately clear.

Introduction

Studies on photoinduced electron transfer (PIET) processes have been vigorously pursued in different laboratories with various basic and applied motivations. During these investigations, it has been increasingly clear that attention needs to be focused on the back-electron-transfer (BET) process as much as on the primary forward-electron-transfer process. A slowing down of the BET rate leads to a better storage of photonic energy. The following strategies may be employed for slowing down the BET rate: (a) employ multiple acceptors such that the initial acceptor transfers the electron quickly to a secondary acceptor, thereby reducing the chance of the electron to return to the donor; (b) compartmentalize the donor and the acceptor in separable microcages, such as micelles, vesicles, or cyclodextrines; (c) control the spin state of the radical pair (RP) formed from the donor−acceptor pair by electron transfer.[1−8]

The last option seems to be particularly attractive. A RP generated by donation of an electron by a donor in its ground state (S_0) to an acceptor in its excited state (S_1 or T_1) should conform to the same spin state as that of the quenched acceptor. For a triplet RP, the BET does not occur until a flip or a rephasing of spin occurs in one of the components of the RP relative to the other.[6] Consequently, the radicals in a triplet-born pair tend to escape from the cage before recombination takes place unless spin-orbit coupling (SOC)-induced recombination in the triplet state is lower. Had the radical pair been born in the singlet state, the BET would occur immediately after the electron transfer. Magnetic fields can cause or prevent the spin reorientation required for converting a reactive singlet RP to an unreactive triplet, or vice versa, and thus can switch on or off the BET rate.[8]

Here, we have focused on the MFE of the radical pair generated by electron transfer to the photoexcited pyrylium salts (**I**−**III**) from the ground state of the donor biphenyl (BP) (**IV**),

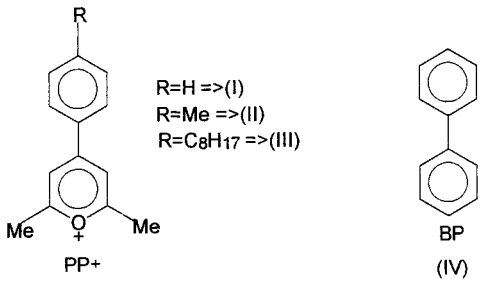

both confined in the same SDS micelle. The choice of our system has been dictated by following considerations.

The Electron Acceptor. (a) Pyrylium salts are good oxidizing agents in the photoexcited state and can act as efficient photosensitizers.[9] These are highly soluble in organic solvents (e.g., dichloromethane) and do not produce any singlet oxygen or super-oxide radical, which might complicate the photochemistry through parallel side reactions. This allows neat conclusions to be drawn regarding reactions of an organic cation.

(b) It may be noted that if a neutral D/A pair is chosen, an electron-transfer reaction leads to a D^+/A^- ion pair in which the Coulombic attractive force lowers the escape rate and thus facilitates the recombination process. However, if an uncharged donor and positively charged acceptors, as above, are chosen, the ionic attractive force between the two components remains absent before or after the electron transfer, thereby reducing the BET rate.[9]

(c) In the pyrylium ion, the quantum yields of the singlet and the triplet are comparable. When the electron donor is present in high concentrations, most of the RPs produced are in the singlet state. Conversely, for lower donor concentrations the singlet quenching is negligible, and the triplet pyrylium becomes the predominant electron acceptor species, generating

† Part of the special issue "Noboru Mataga Festschrift".

* To whom correspondence should be addressed. E-mail: pcmc@mahendra.iacs.res.in.

‡ Indian Association for the Cultivation of Science.

§ Present address: Department of Chemistry and Chemical Technology, Vidyasagar University, Midnapore 721 102, India.

Regional Research Laboratory.

10.1021/jp012561y CCC: $22.00
Published on Web 02/16/2002

triplet RPs only. Thus, both singlet and triplet RPs can be generated depending on the condition. In this article, we concentrate on triplet RPs only.

(d) Last, it is easy to introduce different substitutions in the heterocyclic ring and to change the counter-ion; thus, the reactivities of the different derivatives may be compared with each other.

The Electron Donor. Biphenyl is a nonpolar organic molecule and is likely to stay in the inner hydrocarbon core of the micelle. It easily forms stable $BP^{+\bullet}$ radical by donation of an electron to the photoexcited pyrylium ion.[10] The $BP^{+\bullet}$ radical has an absorption peak at 680 nm, which does not overlap with any triplet or radical absorption due to pyryliums. In a previous communication, we have reported some unusual features in MFE on the donor−acceptor system skatole/TPP^+ (TPP^+ = triphenylpyrylium ion).[11] The TPP-triplet and TPP-radical, however, absorbed at the same wavelength (555 nm) causing some complications in the decay curves. In this case of BP as donor, it is possible to monitor the concentration of $BP^{+\bullet}$ at 680 nm and that of the phenyl pyrylium radical at wavelength below 400 nm; the two decays may, therefore, be compared with each other.

The Micelle. Anionic micelles play a useful role in confining[4] the pyrylium ions in the Stern layer at the periphery and the neutral donor molecule in its interior hydrocarbon core. After electron transfer, the neutral donor molecule becomes charged but the pyrylium radicals become neutral; the latter prefers to go into the interior core of the micelle. The dynamics that ensues following the photoexcitation of the $A^+\cdots D$ system is expected to be different from that of the uncharged $A\cdots D$ pair case. It is interesting to find out whether the dynamics of such a donor−acceptor pair has any effect on MFE. In particular, there is the possibility of the RP recombination taking place at the miceller surface. Theoretical treatments of pair diffusion in various dimensions have shown that geminate reencounters occurring in 3D with a probability of less than 1 have a probability of 1 in systems with two translational degrees of freedom. However, it is difficult to find out exactly the dimension in which the diffusion occurs in the present case.

Experimental Section

2,6-Dimethyl-4-phenyl pyrylium perchlorate and its derivatives have been used after recrystallization from dichloromethane and anhydrous ether twice. Purest grade SDS (Merck) has been used. Biphenyl from Fluka was used after recrystallization from ethanol and water mixture. Triply distilled deionized water is used for the preparation of micellar solutions. All of the solutions are deaerated by purging argon for 30 min. Concentrations employed in the experiment were $[PP^+(\mathbf{I/II/III})] = \sim 5 \times 10^{-4}$ M, $[BP] = \sim 1 \times 10^{-3}$ M, and [SDS] = 0.1 M.

The experiments were carried out in a conventional laser flash photolysis (LFP) setup (Laser Kinetic spectrometer, Applied Photophysics) coupled with a synchronized pulsed electromagnet. The basic circuitry of this setup is described elsewhere.[12] For high-field studies, we have employed a home-built split-coil electromagnet. The pulse current is provided by the discharge of a series of two capacitors (500 μF, 4 kV each) through a mercury ignitron, the latter being triggered by the discharge of another capacitor bank by a synchronously triggered thyristor with the aid of a pulser unit. The pulse duration for the main capacitor bank is about 2 ms. We have ensured that in the time scale of our experiment magnetic field remains constant. The magnetic field was calibrated by using surge-coil technique. For our LFP studies, we have used the third harmonic (355 nm) of an Nd:YAG (DCR-11, Spectra Physics) laser as the pump source and a 250 W pulsed xenon lamp as the monitoring source. The output signal from a photodiode was fed to a digital storage oscilloscope (Tektronix, TDS 350); the subsequent signal processing was done by a personal computer. The transient signal at each wavelength was averaged over 10 shots. The possibility of change in the solution itself brought about by the light flash, the pulsed field, or both was carefully looked into in the following way. The decay curves were obtained for zero field first and then at the highest field with the same freshly prepared degassed solution. The order of the highest- and zero-field experiments was then reversed with the same sample. The results were reproducible. Results on two fresh solutions, identically prepared and degassed, compared very well.

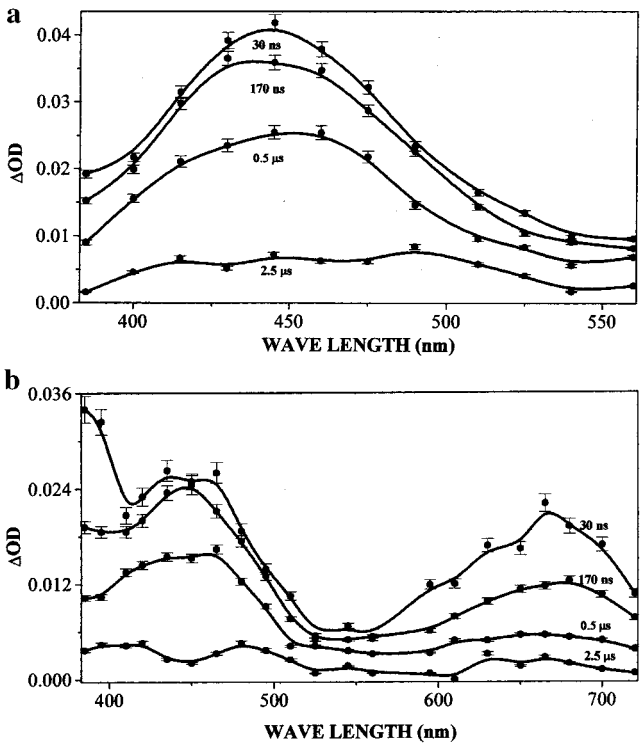

Figure 1. Transient absorption spectrum of compound (**I**) (1×10^{-4} M) in aqueous SDS medium (a) in the absence and (b) × in the presence of BP (1×10^{-3} M).

Results and Discussion

Triplet and Radical Absorption Spectra. The spectra of molecules **I**, **II**, and **III** in neat solvents have been reported in the literature by Gopidas et al.[10] The broad triplet absorption peak occurs at 440 nm in dicholoromethane (DCM) solvent. In our case, the triplet absorption spectrum in SDS medium, shown in Figure 1a, is broader. This is understandable in view of the heterogeneity of the micellar medium and the ionicity of our compound, which makes it soluble in water. Notice that there are transparent windows in triplet absorption at 680 and 385 nm, the former being more transparent than the latter. In the presence of biphenyl (BP), the electron transfer occurs to generate $BP^{+\bullet}$ and $PP^\bullet$ radicals. In neat solvents, $BP^{+\bullet}$ has a band at 680 nm and $PP^\bullet$ (**I**) has one at 385 nm. Similar absorption bands have been observed by us in SDS medium (Figure 1b).

Production of Correlated RPs. Correlated singlet and triplet RPs of $PP^\bullet$ and $BP^{+\bullet}$ are produced on quenching of excited PP^+ by BP. It may be noted that PP^+ when excited by light in the

absence of a quencher produces molecular singlet and triplet states in comparable amounts. For example, the quantum yields of fluorescence of **I**, **II**, and **III** are 0.1, 0.28, and 0.32, respectively, while the triplet quantum yields for the same set of molecules are 0.5, 0.2, and 0.2, respectively.[10] If the quenching of the singlet excited state occurs within the lifetime of the excited PP^+ singlet, the ^1RP is produced. This is expected to happen in the micelle if the quencher BP is located close to the fluorescer. The ^3RP, on the other hand, is produced by comparatively slow diffusion of the quencher from one part to the other. Thus, one can expect that in the miceller system a mixture of ^1RP and ^3RP will be produced, the ratio of the two depending upon the concentration of BP in the micelle. However, the ^1RP immediately recombines, and there is very little magnetic field effect in the time scale of our experiment (MFE on the fluorescence from ^1RP will be discussed elsewhere). The ^3RP takes time to evolve into a singlet state and recombine. In the RP decay curve, one might find the early part magnetically insensitive and the longer of the two decays magnetic field sensitive. Our Figures 2−4 displaying the decay curves as a function of the field do indeed display this feature. It is, however, necessary to point out that the magnetically not-so-sensitive fast decay part could arise also from the $S \rightarrow T_0$ decay at certain fields.

Framework and Mathematical Expressions for RP Decays. We discuss the decay curve of the $PP^{\bullet}/BP^+$ systems within the framework of the Hayashi−Nagakura model.[13] They derived the following expressions for time dependence of the RP assuming a set of competing processes as schematically shown in Scheme 1 (Figure 5). We reproduce here their conclusions.

For triplet-born RPs, the following expressions for decays are pertinent.

I. Case a: $k_P \gg k_0/k_B \gg$ Other Rates

$$B = 0 \text{ T}$$

$$[R] = I_0 \exp(-k_0' t)$$

$$\text{where} \quad k_0' = k_E + k_0$$

$$B \geq B_S \qquad (\text{saturating field, } \sim 0.03 \text{ T})$$

$$[R] = I_f \exp(-k_f t) + I_s \exp(-k_s t)$$

$$\text{where} \quad k_f = k_E + k_B + 2k_R$$

$$k_S = k_E + k_R + k_R'$$

II. Case b: $k_B/k_0 \gg k_P \gg$ Other Rates

$$B = 0 \text{ T}$$

$$[R] = I_0 \exp(-k_0'' t)$$

$$\text{where} \quad k_0'' = k_E + k_p/4$$

$$B \geq B_S$$

$$[R] = I_f \exp(-k_f t) + I_S \exp(-k_S t)$$

$$\text{where} \quad k_f = k_E + k_R + k_R' + k_p/2$$

$$k_S = k_E + k_R + k_R'$$

Here [R] is the total RP concentration in all four sublevels, that is, $[R] = [S] + [T_0] + [T_{+1}] + [T_{-1}]$.

A single-exponential decay curve is expected at zero fields, while for fields greater than that required for making the Zeeman splitting just greater than the hyperfine width of the levels (which is of the order of 0.01 T), double-exponential decays are expected. The field-sensitive rate constants are k_R, k_R', and a part of k_B ($= k_0 + \Delta g\beta B$). Because the field-independent rates (e.g., k_E, k_P, k_0) are much larger than the field-dependent ones (k_R, k_R', $\Delta g\beta B$), the relative change in the fast decay constant is less than that in the slow decay constants. Moreover, the expressions for k_S are the same for both case a and case b, thus making the slow decay constant more convenient to deal with.

Our observed decays of transient absorption are shown in Figures 2−4. The decays at zero-field are nearly single-exponential, but not exactly, which could be due to the heterogeneity of the particular micellar system or to the production of both ^1RP and ^3RP. It is rather tricky to compare the zero-field rate constant, evaluated through a single-exponential expression, with the high-field k_S and k_f, evaluated through a double-exponential expression. We have, therefore, decided not to compare the zero-field curve with other curves in the presence of high field; instead, a curve in the presence of a small field is fitted with a double-exponential expression on the same footing as all other decay curves.[8] For reasons already discussed, only the inverse of the slow component ($1/k_S$) is plotted as a function of the field (Figure 6). It is, however, better to plot the more directly observable radical yield (measured by the $A(t)$ value normalized by dividing by the peak value of A at initial times) at a specified time delay as a function of the field (Figure 7). Our choice of a 3 μs time delay is arbitrary; however, the same qualitative pattern emerges if we choose the time delay of 0.7 μs (where the sensitivity to the field is maximum) or the time delay of 6 μs (where the sensitivity to the field is minimum). It may be observed that the RP lifetime ($1/k_S$) vs B curves (Figure 6) and the yield vs B curves (Figure 7) qualitatively agree with each other. In view of the uncertainties in the estimate of k_S, we attach greater importance to the yield vs B curves where small differences become immediately obvious.

Comparison between the Decays of the Two Component Radicals. We have chosen two wavelength windows at 680 and 385 nm to monitor $BP^{+\bullet}$ and $PP^{\bullet}$ radicals, respectively, as a function of time. For the RP system, $BP^{+\bullet}/PP^{\bullet}$ (**I**), the decay of $BP^{+\bullet}$ at 680 nm (Figure 2a) is compared with the decay of $PP^{\bullet}$ (**I**) at 385 nm (Figure 2c). It may be noticed that the decays at both windows are similar. However, some differences, although small, do exist. One difference is that at long times the $A(t)$ value becomes very small at 680 nm signifying almost zero yield for $BP^{+\bullet}$, whereas it attains a steady higher value at 385 nm signifying a small but greater yield for $PP^{\bullet}$. This difference could, of course, be a reflection of the fact that at 385 nm the relatively long-lived unquenched molecular triplet also absorbs. The presence of a long-lived triplet should not matter in the measurement of lifetime. The variation of lifetimes with B is shown in Figure 6. The observed general similarity between $PP^{\bullet}$ and $BP^{+\bullet}$ decays is expected. Because the escape from the cage occurs when either of the two radicals leaves the micellar cage, the total escape rate is the sum of the disappearance rates for the two radicals. If the recombination occurs only between two radicals of two different types and not between the radicals of the same type, their overall recombination rates may be expected to remain the same. The close similarity between the two decays (680 and 385 nm), therefore, means that there is no extensive reaction between radicals of the same type. The small noticeable differences that exist between the two sets of curves are being further analyzed by us.

To vary the escape rate we have attached a long-chain C_8H_{17} to the PP^+ ion with the intention of anchoring it to the micelle.

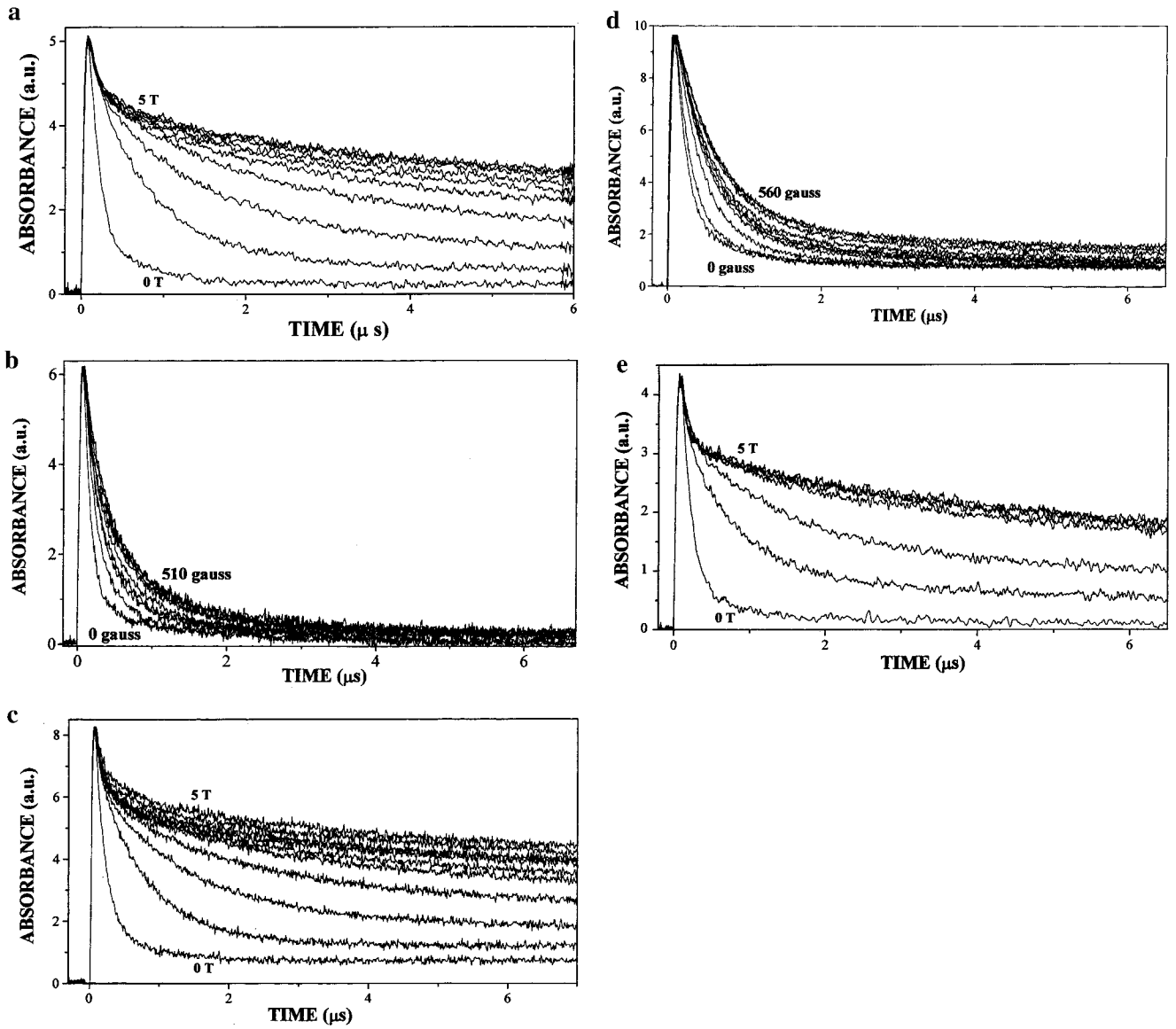

Figure 2. Decay of transient observed at 680 nm for compound **I**/BP system in the presence of (a) various external high fields and (b) various external low fields, decay of transient observed at 385 nm for compound **I**/BP system in the presence of (c) various external high fields and (d) various external low fields, and (e) decay of transient observed at 680 nm for compound **I**/BP system containing 0.1 M $NaClO_4$ in the presence of various external high fields.

However, we could not see any perceptible difference in the overall zero-field escape rate between **II** and **III**. The equality of the escape rate for **II** and **III** means that the sum is dominated by the $BP^{+\bullet}$ escape rate, possibly the larger of the two. It may be noticed from the decay curve for **I** (Figure 2a) that there is insignificant yield of escape radicals at zero field, which means that most of the radicals generated on the micellar surface by the laser pulse recombine before escaping. In other words, the recombination is much faster than the escape rate in the absence of the field. We, therefore, compare the decay curves of the two RPs in the presence of a small field, 10 mT, where there is a measurable positive yield of the free radicals.

Magnetic Field Effect on Yields of Free Radicals and Lifetime of RPs. The lifetime (inverse of k_s) vs B and the yield (at 3 μs delay) vs B curves are displayed in Figures 6 and 7, respectively. The yield (at 0.7 μs delay) is plotted as a function of B in Figure 8, and the inset shows the yield vs B plot for very low fields generated with a small home-built steady-field magnet. A large effect was observed for compound **I**, the escape yield at 5 T being about 20 times the zero-field value at a long time delay (see also Figures 2a and 7). It is apparent from a plot of the rate of increment of yield with increment of field H (Gauss), $\Delta y/\Delta H$, against $\log_e H$ (Figure 10) that more than one mechanism is at work. At low fields, the dominant mechanism is the HFC one. When the Zeeman separation exceeds the hyperfine width, only the $S \leftrightarrow T_0$ channel remains open and the $S \leftrightarrow T_\pm$ channels stop functioning because of the removal of the $S,T_\pm$ degeneracy. Thus, the intersystem-crossing rate is reduced to one-third leading to lengthening of the RP lifetime. The $B_{1/2}$ or the field at which the field-induced change is half the saturation value (the low-field one, in this case; see Figure 8, inset) should depend on the average hyperfine interaction. We have calculated the latter quantitatively using semiempirical INDO-UHF method for the compounds **I** and **II**. The magnitude comes out to be very close to the experimental value. The isotropic HFC (hyperfine coupling) mechanism saturates out at fields greater than 10 mT.

At high fields, the mechanisms that could be relevant are the Δg mechanism (ΔgM) and the relaxation mechanism (RM).[8,13] However, the two mechanisms have different field dependences. For a ^{3}RP, the $T_\pm \leftrightarrow S_0$ relaxation slows down with field. On the other hand, the ΔgM increases the $T_0 \leftrightarrow S$ interconversion

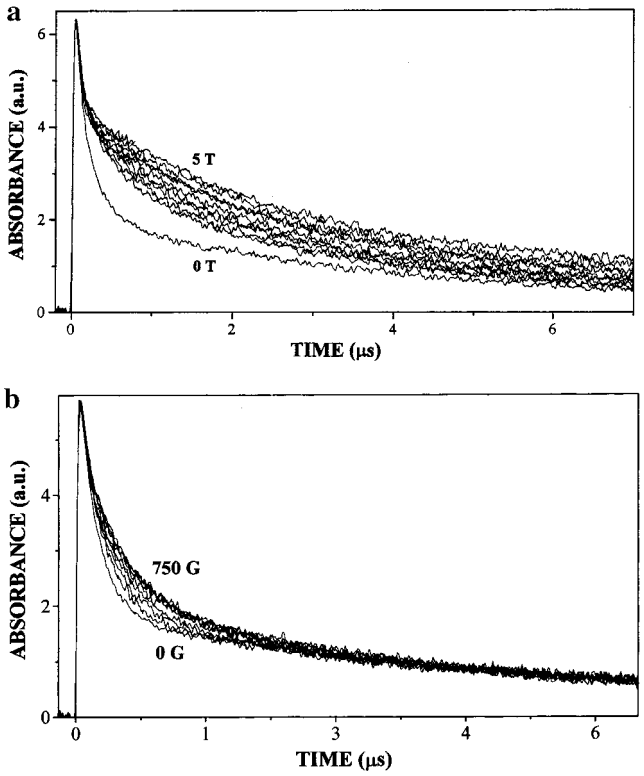

Figure 3. Decay of transient observed at 680 nm for compound **II**/BP system in the presence of (a) various external high fields and (b) various external low fields.

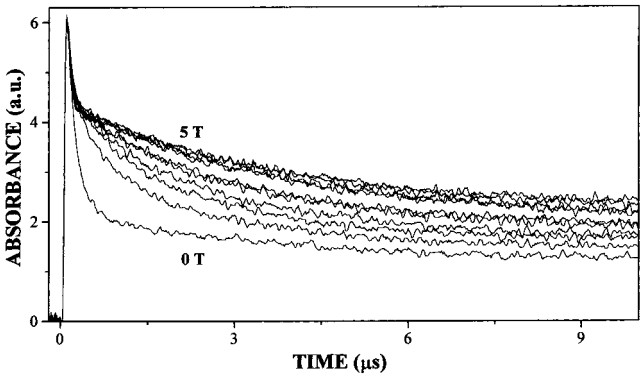

Figure 4. Decay of transient observed at 680 nm for compound **III**/BP system in the presence of various external high fields.

with field and thus reduces the lifetime of the ^{3}RP until the (S, T_0) spin equilibrium is reached. Because in the $BP^{+\bullet}/PP^{\bullet}$ system we have observed the ^{3}RP lifetime to increase with field without any reversion, we conclude that the ΔgM is not playing an important role in this case, at least not up to a 5 T field. Hayashi et al.[8] have suggested a simple experimental method of separating the effect of the ΔgM from that of the RM. When Gd^{3+} ion is added, it causes rapid spin relaxation (S $\leftrightarrow$ $T_{\pm}$) by coupling through the spin−spin exchange interaction with one of the partners of the RP. They observed that the ΔgM contribution remained unaffected by the addition Gd^{3+} but the RM contribution got quenched. When we applied this test to the present system, we found that the MFE is almost totally quenched (Figure 9) in the presence of 4 mM Gd^{3+}. The isotopic ΔgM, therefore, is indeed not very relevant for the discussion of the trends of MFEs observed in this study.

We have tried to understand the behavior at high fields in the framework of the relaxation mechanism,[8,13] although alternative approaches exist.[14] At approximately zero field, the

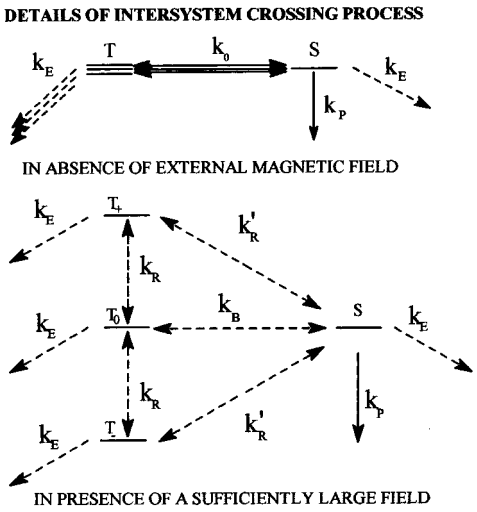

Figure 5. Energy levels of a radical pair with $J = 0$ and various rate constants in different external fields.

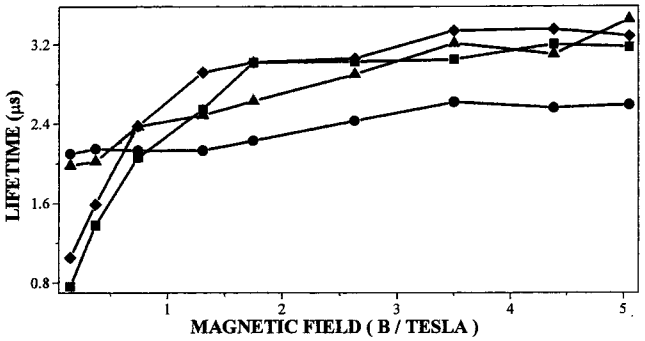

Figure 6. Plot of lifetime of radical pairs as a function of magnetic field: (■) compound **I** at 680 nm; (◆) compound **I** at 385 nm; (●) compound **II** at 680 nm; (▲) compound **III** at 680 nm.

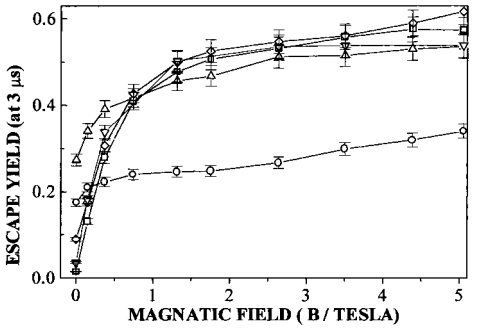

Figure 7. Plot of escape yield of radical pairs as a function of magnetic field: (□) compound **I** at 680 nm; (◇) compound **I** at 385 nm; (○) compound **II** at 680 nm; (△) compound **III** at 680 nm; (▽) compound **I** at 680 nm in the presence of 0.1 M $NaClO_4$.

relaxation from singlet to triplet or vice versa is fast, leading to a fast decay of a triplet-born RP. An increase of field leads to slowing down of the (S, T_0) $\leftrightarrow$ $T_{\pm}$ relaxation leading to a lengthening of lifetime of the ^{3}RP. The relaxation in a RP can occur by tumbling of a molecule in an anisotropic field defined by spin dipole−spin dipole interaction, hyperfine field, *g*-field, or a combination of these. The *d*−*d* interaction depends on the inverse of sixth power of the interradical distance; these are important for lifetime consideration of linked biradicals but may be ignored in micelles where the average distance between the two radicals is large. In the present case, one radical is localized in the core of the micelle and the other at the periphery, and hence, for the ^{3}RP under consideration, the *d*−*d* interaction may be neglected.

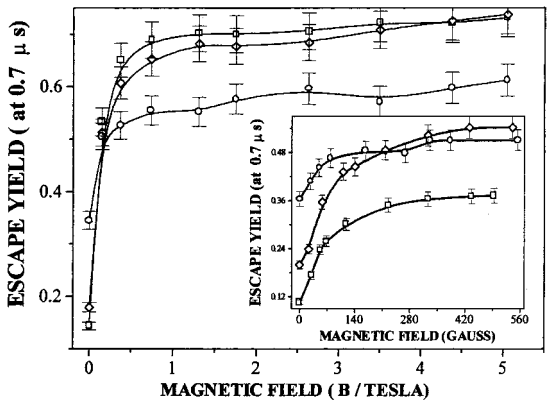

Figure 8. Plot of escape yield of radical pairs as a function of magnetic field: (□) compound **I** at 680 nm; (◇) compound **I** at 385 nm; (○) compound **II** at 680 nm. The inset represents the corresponding low-field plots.

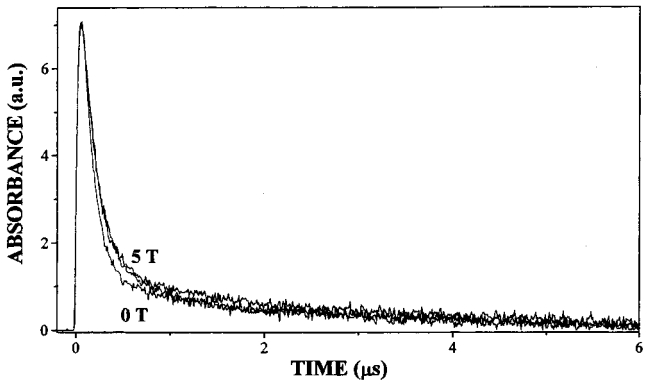

Figure 9. Decay of transient observed at 385 nm for compound **I**/BP system containing 4 mM Gd^{3+} salt in the presence of various external high fields.

If we leave out the dipole−dipole interaction as a possible mechanism of relaxation for a RP encased in a micelle, the lifetime of a caged RP may be obtained from the following expression:[8]

$$\frac{1}{\tau} = \sum_{i=1,2}\left[2\pi^2\beta^2\left\{(\delta g_i)^2B^2 + \frac{20}{9}g_i^{\,2}(H_i^{\mathrm{loc}})^2\right\}\frac{\tau_i^{\mathrm{c}}}{5h^2(1+\gamma_i^{\,2}B^2\tau_i^{\mathrm{c}2})}\right] + K_{\mathrm{T}}$$

Here g_i and γ_i are the g value and the magnetogyric ratio of the electron on each of the radicals, respectively; the parameter τ_i^{c} is the rotational correlation time of the radical i; H_i^{loc} and δg_i are the parameters for the anisotropic *hf* tensor and the anisotropic g-tensor of the radical i, respectively. In this expression if $\gamma^2B^2\tau_{ci}^2 \ll 1$, the contribution of the first term increases with B and, as a consequence, the lifetime decreases. If $\gamma^2B^2\tau_{ci}^2 \gg 1$, the first term leads to saturation. The second term, on the other hand, decreases with B, and hence, the lifetime increases with B. The third term, k_{T}, is a field-independent empirical parameter that is necessary for a good fit and is interpreted as the triplet decay rate. While qualitatively the general nature of the τ vs H_{ex} curve is understood, it is not possible to extract reliable parameters out of the observed decays. We would only like to point out that the shape of the τ vs B curve is consistent with a lower δg parameter compared to the benzil-SDS system investigated by us before.[15] It has been shown by Fujiwara et al.[16] through extensive simulation with different values of the parameters δg and τ_{c} that the smaller the δg parameter is the higher the lifetime increases with field. The large increase of lifetimes with field in the present case is consistent with a lower value of the δg parameter for the radicals.[8]

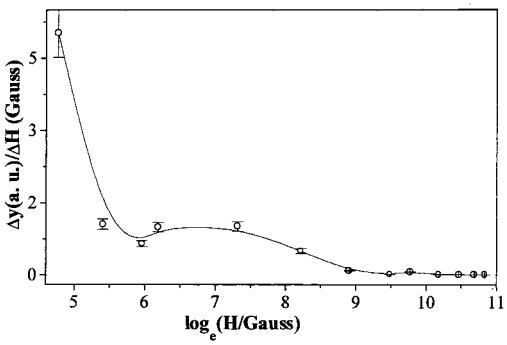

Figure 10. Plot of the ratio of change of escape yield (Δy) per unit change of magnetic field (ΔH) (Gauss) vs logarithm of magnetic field (Gauss) for compound **I** at 680 nm.

MFE on a ^{3}RP, measured by the percentage increase in yields of free radicals on application of a 5 T field, decreases considerably on substituting the H atom at the para position of PP^+ with a methyl group. Our calculation shows that the average hyperfine couplings in the two radicals generated from **I** and **II** are nearly the same. Another possibility is that the methyl rotation, just like spin−orbit coupling, causes field-independent spin relaxation and thus reduces the relative contribution of the field-dependent spin relaxation. However, methyl rotation would have made the zero-field lifetime of the methyl-substituted compound (**II**) shorter than the H-substituted compound, which is clearly not the case. It is likely that additional factors such as the J-integral difference between the two cases are at work. We shall address this problem in a later communication.

MFE in the Presence of $NaClO_4$. We have carried out MFE studies in the presence of 0.1 M $NaClO_4$ in SDS micellar medium. Salts are known for their capability of increasing the micellar size. In one of our previous studies with benzil-SDS radical pair,[15] we reduced the micellar size and increased the escape rate of the radical by adding dioxane to the micellar solution and noticed that the inversion in high fields become less pronounced. The purpose of adding the salt in the present study was to make the micelle larger and thereby reduce the escape rate so that the saturation and inversion effect could be more clearly seen. The qualitative feature of the MDF curve in the absence of salt is retained here (compare Figure 2, parts a and e). In the presence of the salt, the high-field saturation occurs at about 1.5 T instead of at 3.5 T observed without $NaClO_4$.

Summary and Concluding Remarks

We have investigated the magnetic field effect (MFE) on the radical pairs (RPs) generated by the photoexcitation of the phenyl pyrylium ion (PP^+) in the presence of the electron donor, biphenyl. The lifetimes of the RPs and the yields of the free radicals increase considerably with field. The rate of increase of yield with field is maximum at the lowest field, but it reaches a minimum at fields on the order of 50 mT; then it slightly rises again and remains steady before decreasing to zero at 1.1 T. The low-field variation of MFE conforms to the pattern expected for the isotropic HFC mechanism, and the high-field variation conforms to that expected for the relaxation mecha-

nism. The low-field MFE maintains a constant relation with the high-field MFE. This indicates that, out of the different interactions that lead to relaxation, the anisotropic HFC plays the major role. The magnitude of MFE is the highest for the unsubstituted $PP^{\bullet}$ (**I**). Although this may indicate that the H atom at the para position of the phenyl ring (**I**) is responsible for high HFC, our calculation shows that the average hyperfine field for **I** and **II** are nearly the same. The reason for the methyl group effect is not immediately clear to us. Addition of salt causes saturation at a slightly lower field, presumably because of a reduction in the escape rate of $PP^{\bullet}$ from the micellar cage.

The pyrylium salts are widely used in organic synthesis involving photosensitizers. Apart from producing organic cation radicals in the laboratory required for various synthesis, they are useful in electrophotography, polymerization, and phototherapy. It should be possible to influence the courses of all of these reactions by controlling the yields of free radicals by varying the magnetic field. The effect of the field on the yields is indeed large for the $PP^{\bullet}$ (**I**) radical. Because of the large magnitude of MFE, it might be an ideal candidate for investigating the relation between the MFE and the size of the reverse micelle. A thorough electron paramagnetic resonance (EPR) investigation on these systems may throw further light on the spin evolution process of these RPs.

References and Notes

(1) Atkins, P. W.; Lambert, T. P. *Annu. Rep. Prog. Chem., Sect. A* **1975**, *72*, 67.

(2) Boxer, S. G.; Chidsey, C. E. D.; Roelofs, M. G. *Annu. Rev. Phys. Chem.* **1983**, *34*, 389.

(3) Buchachenko, A. L. *Prog. React. Kinet.* **1984**, *131*, 163.

(4) Gould, I. R.; Turro, N. J.; Zimmt, M. B. *Adv. Phys. Org. Chem.* **1984**, *1*, 20.

(5) Salikhov, K. M.; Molin, Y. N.; Sagdeev, R. Z.; Buchachenko, A. L. *Spin Polarisation and Magnetic Field Effects in Radical reactions*; Elsevier: Amsterdam, 1984.

(6) Steiner, U. E.; Ulrich, T. *Chem. Rev.* **1989**, *89*, 51.

(7) Bhattacharyya, K.; Chowdhury, M. *Chem. Rev.* **1993**, *93*, 507.

(8) Nagakura, S., Hayashi, H., Azumi, T., Eds. *Dynamic Spin Chemistry*; Kodansha, Tokyo and John Wiley & Sons: New York, 1998.

(9) Miranda, M. A.; Garcia, H. *Chem. Rev.* **1994**, *94*, 1063.

(10) Monoj, N.; Ajit Kumar, R.; Gopidas, K. R. *J. Photochem. Photobiol. A* **1997**, *109*, 109.

(11) Haldar, M.; Chowdhury, M. *Chem. Phys. Lett.* **2000**, *319*, 449.

(12) Misra, A.; Dutta, R.; Nath, D. N.; Sinha, S.; Chowdhury, M. *J. Photochem. Photobiol. A* **1999**, *96*, 155.

(13) Hayashi, H.; Nagakura, S. *Bull. Chem. Soc. Jpn.* **1984**, *57*, 322.

(14) Hansen, M. J.; Newfield, A. A.; Pederson, J. B. *Chem. Phys*. **2000**, *260*, 125.

(15) Misra, A.; Halder, M.; Chowdhury, M. *Chem. Phys. Lett*. **1999**, *305*, 63.

(16) Fujiwara, Y.; Aoki, T.; Yoda, K.; Cao, H.; Mukai, M.; Haino, T.; Fukazawa, Y.; Tanimoto, Y.; Yonemura, H.; Matsuo, T.; Okazaki, M. *Chem. Phys. Lett*. **1996**, *259*, 361.